U.S. ARMY

RESEARCH LABORATORY

Heat Transfer in Conical Corner and Short Superelliptical Transition Ducts

Philip Poinsatte
Glenn Research Center, Cleveland, Ohio

Douglas Thurman
U.S. Army Research Laboratory, Glenn Research Center, Cleveland, Ohio

Steven Hippensteele
Glenn Research Center, Cleveland, Ohio

NASA STI Program . . . in Profile

Since its founding, NASA has been dedicated to the advancement of aeronautics and space science. The NASA Scientific and Technical Information (STI) program plays a key part in helping NASA maintain this important role.

The NASA STI Program operates under the auspices of the Agency Chief Information Officer. It collects, organizes, provides for archiving, and disseminates NASA's STI. The NASA STI program provides access to the NASA Aeronautics and Space Database and its public interface, the NASA Technical Reports Server, thus providing one of the largest collections of aeronautical and space science STI in the world. Results are published in both non-NASA channels and by NASA in the NASA STI Report Series, which includes the following report types:

- TECHNICAL PUBLICATION. Reports of completed research or a major significant phase of research that present the results of NASA programs and include extensive data or theoretical analysis. Includes compilations of significant scientific and technical data and information deemed to be of continuing reference value. NASA counterpart of peer-reviewed formal professional papers but has less stringent limitations on manuscript length and extent of graphic presentations.

- TECHNICAL MEMORANDUM. Scientific and technical findings that are preliminary or of specialized interest, e.g., quick release reports, working papers, and bibliographies that contain minimal annotation. Does not contain extensive analysis.

- CONTRACTOR REPORT. Scientific and technical findings by NASA-sponsored contractors and grantees.

- CONFERENCE PUBLICATION. Collected papers from scientific and technical conferences, symposia, seminars, or other meetings sponsored or cosponsored by NASA.

- SPECIAL PUBLICATION. Scientific, technical, or historical information from NASA programs, projects, and missions, often concerned with subjects having substantial public interest.

- TECHNICAL TRANSLATION. English-language translations of foreign scientific and technical material pertinent to NASA's mission.

Specialized services also include creating custom thesauri, building customized databases, organizing and publishing research results.

For more information about the NASA STI program, see the following:

- Access the NASA STI program home page at *http://www.sti.nasa.gov*

- E-mail your question via the Internet to *help@ sti.nasa.gov*

- Fax your question to the NASA STI Help Desk at 301–621–0134

- Telephone the NASA STI Help Desk at 301–621–0390

- Write to:
  NASA Center for AeroSpace Information (CASI)
  7115 Standard Drive
  Hanover, MD 21076–1320

Heat Transfer in Conical Corner and Short Superelliptical Transition Ducts

Philip Poinsatte
Glenn Research Center, Cleveland, Ohio

Douglas Thurman
U.S. Army Research Laboratory, Glenn Research Center, Cleveland, Ohio

Steven Hippensteele
Glenn Research Center, Cleveland, Ohio

June 2008

Level of Review: This material has been technically reviewed by expert reviewers.

Available from

Heat Transfer in Conical Corner and Short Superelliptical Transition Ducts

Philip Poinsatte
National Aeronautics and Space Administration
Glenn Research Center
Cleveland, Ohio 44135

Douglas Thurman
U.S. Army Research Laboratory
Glenn Research Center
Cleveland, Ohio 44135

Steven Hippensteele
National Aeronautics and Space Administration
Glenn Research Center
Cleveland, Ohio 44135

Summary

Local surface heat transfer measurements were experimentally mapped using a transient liquid-crystal heat-transfer technique on the surface of two circular-to-rectangular transition ducts. One has a transition cross section defined by conical corners (Duct 1) and the other by an elliptical equation with changing coefficients (Duct 2). Duct 1 has a length-to-diameter ratio of 0.75 and an exit plane aspect ratio of 1.5. Duct 2 has a length-to-diameter ratio of 1.0 and an exit plane aspect ratio of 2.9.

Test results are reported for various inlet-diameter-based Reynolds numbers ranging from 0.45×10^6 to 2.39×10^6 and two free-stream turbulence intensities of about 1 percent, which is typical of wind tunnels, and up to 16 percent, which may be more typical of real engine conditions.

Introduction

A continuing objective in jet engine technology is higher engine efficiency. One method of obtaining higher efficiency is the use of higher engine operating temperatures and pressures. The resulting higher turbine-inlet temperatures and pressures increase the importance of knowing the temperatures on the gas path surfaces.

Some recent designs of jet engine exhaust ducts and nozzles for military aircraft have moved away from round exits. These newly designed exits often involve rectangular or more irregular shapes. These new designs have two main areas of benefit: lower observable infrared signatures from nozzles and increased performance through vectoring of exhaust nozzles. In a jet engine these new designs require a transition duct going from the round cross section turbine exit to the rectangular cross section nozzle.

This changing of flow path geometry coupled with efforts to increase engine operating temperature leads to concerns about items such as drag and metal surface temperature. In an effort to keep the weight down, the ducts should be kept as short as possible; however, short ducts may lead to flow separation and thus viscous losses and potential hot spots. Therefore, accurate knowledge of flow characteristics and heat transfer is helpful in design of low-weight, short ducts.

The present work concentrates on heat transfer measurements on two round-to-rectangular duct designs. The ducts employed in these tests were similar in geometry to transition ducts that were tested aerodynamically by NASA personnel and NASA contractors: C. Spuckler (ref. 1: personal communication, NASA Glenn Research Center, Cleveland, OH, 2003.) and Buck (ref. 2) conducted aerodynamic and cooling performance measurements on the same general geometry as Duct 1. Patrick and McCormick (ref. 3) conducted laser velocimetry and pressure measurements on the Duct 2 design.

Symbols

a, b	duct geometry constants in table II equation
c	specific heat at constant pressure
D	diameter
h	heat transfer coefficient
k_a	thermal conductivity of air
k_w	thermal conductivity of duct wall
n	duct geometry exponent in table II equation
Nu	Nusselt number
Nu_0	Nusselt number for turbulent flow in a circular pipe
Pr	Prandtl number, $c\mu/k_a$
R	duct corner radius shown in figures 3 and 5
Re	Reynolds number based on duct inlet diameter
T_i	initial duct temperature
T_r	recovery air temperature
T_s	duct-surface temperature
Tu	free-stream turbulence intensity

t	time
β	nondimensional time, $h t^{1/2}/(\rho c k_w)^{1/2}$
θ	nondimensional temperature, $(T_i - T_s)/(T_i - T_r)$
ρ	density
μ	viscosity
x	duct coordinate, streamwise
y	duct coordinate
z	duct coordinate

Experimental Technique

Tests were conducted in the Transition Duct Heat Transfer Tunnel in the Engine Research Building (ERB), SW–2, at the NASA Glenn Research Center, employing a transient liquid crystal technique to measure heat transfer coefficients. The ducts were tested independently. The experimental method and facility are described fully in reference 4 and are briefly outlined below.

The method (Jones and Hippensteele (ref. 5) and Carslaw and Jaeger (ref. 6)) involves preheating a duct to a uniform temperature of nominally 65.4 °C (150 °F) before allowing room temperature air to be suddenly drawn through it. As the surface cooled, the resulting isothermal contours on the duct surface were revealed using a surface coating of thermochromic liquid crystals that display distinctive colors at particular temperatures. A video record was made of the temperature and time data for all points on the duct surfaces during each test. Using this surface temperature-time data together with the temperature of the air flowing through the model and the

initial temperature of the model wall, the heat transfer coefficient can be calculated by assuming one-dimensional conduction out of a semi-infinite wall. The solution for the case of a step change in flow gives the nondimensional surface temperature as a function of nondimensional time through the complimentary error function as follows:

$$\theta = 1 - e^{\beta^2}\,\text{erfc}(\beta) \tag{1}$$

θ and β are the nondimensional temperature and time, respectively, defined as

$$\theta = \frac{T_i - T_s}{T_i - T_r} \tag{2}$$

$$\beta = \frac{h\sqrt{t}}{\sqrt{\rho k_w}} \tag{3}$$

where T_i is the initial surface temperature, T_s is the duct wall surface temperature indicated by the liquid crystal and T_r is the air recovery temperature. Additionally, h is the heat transfer coefficient and t is the time from airflow start. Also, ρ is the density, c is the specific heat, and k_w is thermal conductivity; these are material properties of the duct wall. Hence it can be seen that if the duct wall thermal properties, air temperature and initial surface temperature are known, the heat transfer coefficients can be found for a given time and liquid crystal temperature.

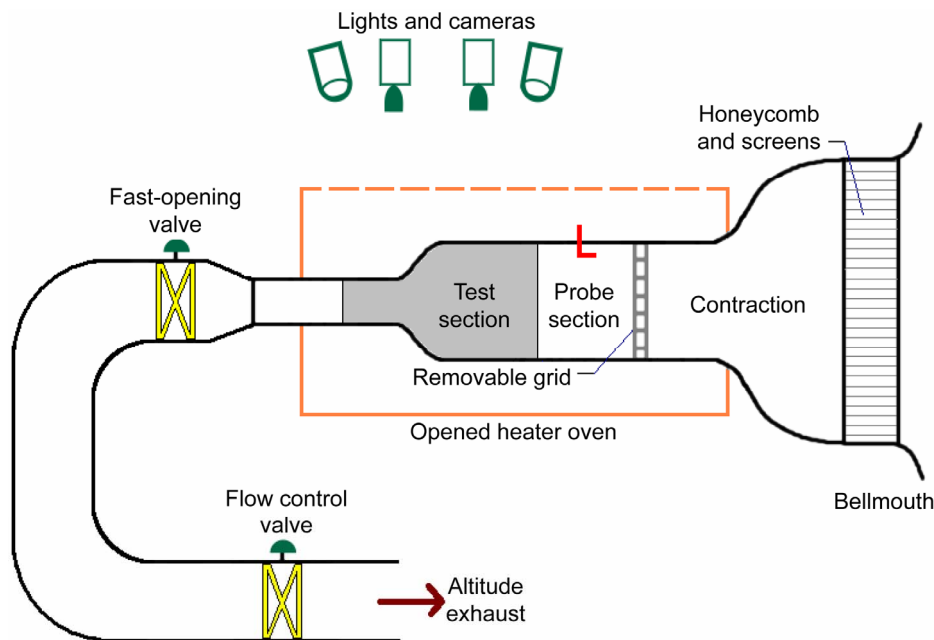The tunnel (fig. 1) consists of an open, room air inlet bellmouth, flow conditioning screens and honeycomb, 12:1 are

Figure 1.—NASA Glenn Engine Research Building SW–2 Transition Duct Heat Transfer Tunnel.

contraction, pressure probe section, high-turbulence-generating grid (when used), and the particular transition duct being tested. The air passed through a straight downstream section, an exit adapter section, a fast-opening 30.5-cm (12-in.) round valve, a flow-control valve, and into the central altitude exhaust (vacuum) system. The exit adapter section attached the transition duct sections to the fast-opening valve. With the fast-opening valve closed (before the test was run) the flow control valve was set to produce the desired flow conditions through the test duct. At the beginning of the test, the fast-opening valve opened to produce a near step change in the flow startup condition. A microswitch on the fast valve produced an electrical signal that was recorded by the data acquisition system to indicate the airflow start time. Prior to the test, the duct surfaces were uniformly heated using two heating systems; the first was an automatic temperature-controlled heater blanket completely surrounding the test duct like an oven, and the second was an internal hot-air loop through the inside of the test duct. The temperature nonuniformity of the test duct model wall was held very small. The time-dependent images of the liquid crystal colors were seen by RGB (red-green-blue) video cameras and were recorded on Betacam SP (Sony Corporation) video tape recorders.
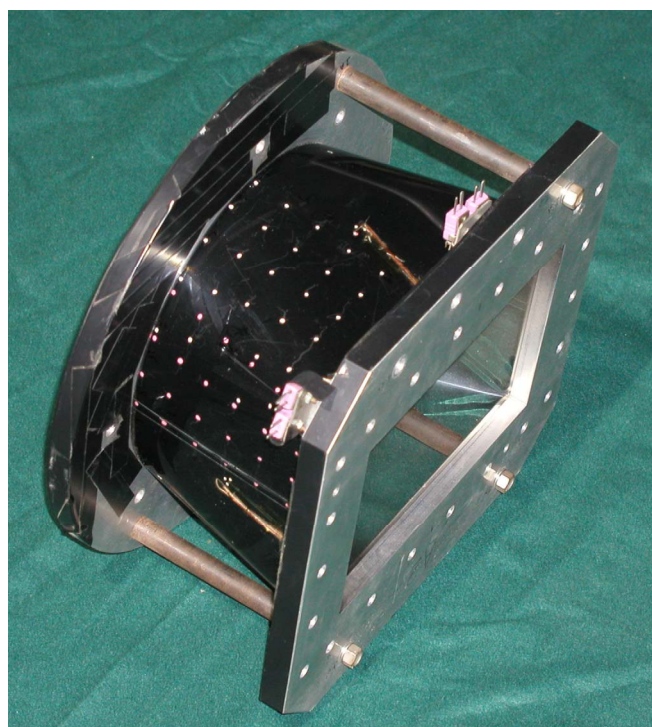
For the test runs, the inlet airflow was typically at room temperature and atmospheric pressure. Flow rates ranged from 1.36 to 7.26 kg/s (3 to 16 lb/s), Mach number from 0.09 to 0.56, and inlet Reynolds number based on the duct inlet diameter from 0.45×10^6 to 2.39×10^6. The Prandtl number was nominally 0.71.

Test Models

Two acrylic round-to-rectangle transition ducts were tested. Heat transfer data were taken from one quadrant of each duct. Each model was marked with two grids in the data quadrant, which aided in the image processing. See reference 4 for details on data reduction.

Duct 1 has a round 22.23-cm (8.75-in.) diameter inlet and a 24.28- by 16.03-cm (9.56- by 6.31-in.) rectangular exit. The transition from round to rectangle is defined mathematically by the composite shape of four quarter conic sections, each of whose base forms one quadrant of the inlet circle and whose vertex forms the rectangular exit corner corresponding to the same quadrant. The overall length is 16.66 cm (6.56 in.). Duct 1 is shown in figure 2, and the coordinates for Duct 1 are given in table I.

Figure 2.—Duct 1: Conical corner.

TABLE I.—DUCT 1 SURFACE COORDINATES[a]

Coodinate, x	Coodinate, y	Coodinate, z	Corner radius, R
0.000	0.000	0.000	4.375
0.250	0.186	0.122	4.205
0.500	0.371	0.243	4.036
0.750	0.557	0.365	3.866
1.000	0.742	0.486	3.696
1.250	0.928	0.608	3.527
1.500	1.114	0.729	3.357
1.750	1.299	0.851	3.188
2.000	1.485	0.972	3.018
2.250	1.670	1.094	2.848
2.500	1.858	1.215	2.679
2.750	2.041	1.337	2.509
3.000	2.227	1.458	2.339
3.250	2.413	1.580	2.170
3.500	2.598	1.701	2.000
3.750	2.784	1.823	1.831
4.000	2.969	1.944	1.661
4.250	3.155	2.066	1.491
4.500	3.341	2.188	1.322
4.750	3.526	2.309	1.152
5.000	3.712	2.431	0.982
5.250	3.897	2.552	0.813
5.500	4.083	2.674	0.643
5.750	4.268	2.795	0.474
6.000	4.454	2.917	0.304
6.250	4.640	3.038	0.134
6.448	4.787	3.135	0.000

[a]Coordinate system is shown in figure 3.
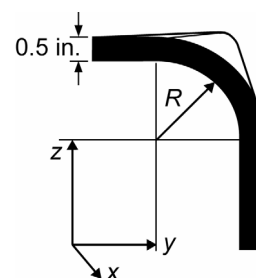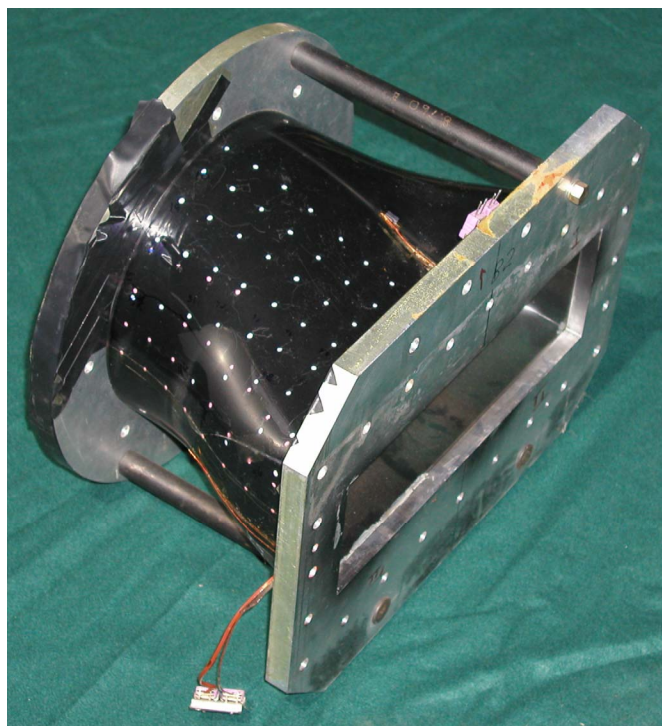

Figure 3.—Coordinate system for Duct 1.

Figure 4.—Duct 2: Short superellipse.

TABLE II.—CONSTANTS FOR DUCT 2
GEOMETRY EQUATION[a]
$(y/a)^n + (z/b)^n = 1$

Coordinate, x	Geometry constant, a	Geometry constant, b	Geometry exponent, n
0.0	4.375	4.375	Circle
0.5	4.389	4.362	2.00
1.0	4.430	4.323	2.00
1.5	4.499	4.258	2.00
2.0	4.597	4.165	2.00
2.5	4.724	4.045	2.00
3.0	4.882	3.896	2.03
3.5	5.073	3.717	2.08
4.0	5.298	3.506	2.17
4.5	5.558	3.262	2.34
5.0	5.802	3.034	2.60
5.5	6.010	2.839	2.97
6.0	6.184	2.676	3.49
6.5	6.326	2.541	4.30
7.0	6.439	2.435	5.58
7.5	6.522	2.356	8.00
8.0	6.577	2.304	13.7
8.5	6.605	2.278	35.9
8.75	6.608	2.275	Rectangle

[a]Coordinate system is shown in figure 5.

Figure 5.—Coordinate system for Duct 2.

Duct 2 consists of a round inlet of diameter 22.23 cm (8.75 in.) and a rectangular cross section of 11.43 by 33.66 cm (4.50 by 13.25 in.). Duct 2 is shown in figure 4; its transition cross section is defined by a changing elliptical shape described by the equation and coefficients in table II. The overall duct length is 22.23 cm (8.75 in.).

Results and Discussion

Inlet flow surveys of the tunnel were previously measured (ref. 4) using a total pressure probe and a boundary layer probe. Measurements were taken at the probe section just upstream of the duct inlet. These measurements have shown mean velocity profiles, law of wall profiles, and boundary layer parameters that are generally consistent with turbulent flow.

Turbulence measurements were previously made using a commercial hot wire system. In the open tunnel cases (no grid), the measured turbulence intensities for various Reynolds numbers were nominally 1 percent. For the cases with the turbulence-generating grid installed, the turbulence intensities were measured to be around 16 percent near the duct inlet. This turbulence matched values from the Baines and Peterson (ref. 7) correlation and was expected to decay according to the correlation.
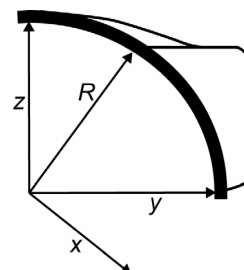
Figure 6 shows aerodynamic data taken at the exit plane of Duct 1. These measurements were taken by Spuckler (ref. 1) and are included here to illustrate some flow characteristics typical of short circular-to-rectangular transition ducts. The left side shows contours of normalized mean flow velocity. The right side shows the normalized secondary velocities. The graph shows that as the top and bottom duct walls converge, the flow is pushed inward. As the side duct walls diverge, the flow spreads out.

Heat transfer measurements were made for high and low turbulence cases at various Reynolds numbers. Heat transfer coefficients were calculated using equations (1) to (3). Heat transfer measurements were made dimensionless by calculating the Nusselt number as follows:

$$\mathrm{Nu} = \frac{hD}{k_a} \tag{4}$$

where D is inlet diameter and k_a is thermal conductivity of the air. Results are also presented as Nusselt number normalized by values for turbulent flow in a pipe given by the correlation

$$\mathrm{Nu}_0 = 0.023\left(\mathrm{Re}^{0.8}\right)\left(\mathrm{Pr}^{0.4}\right) \tag{5}$$
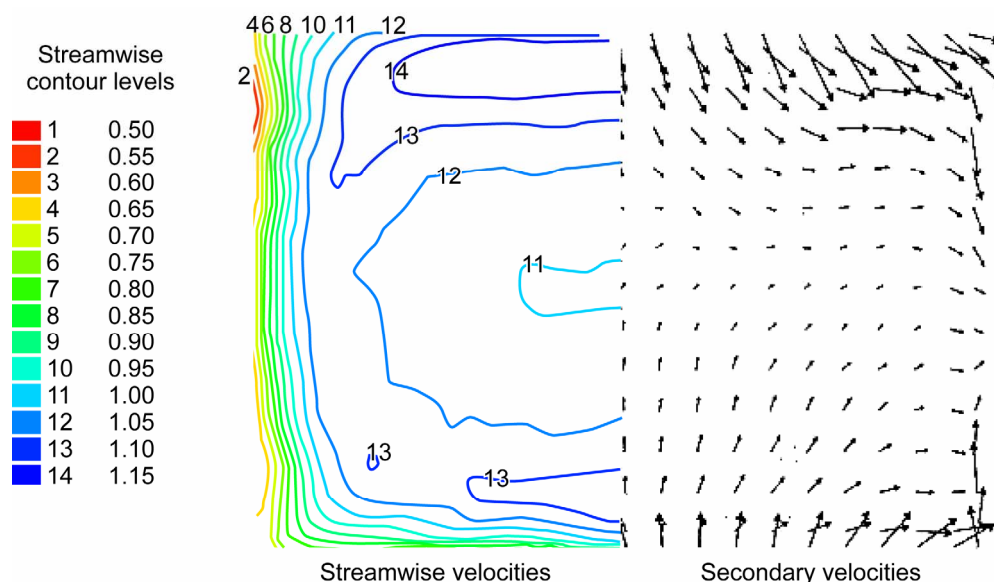
Figure 6.—Duct 1 exit veloctiy profile normalized by inlet velocity. Nominal inlet Mach number is 0.5 (from ref. 1).

where Re is the Reynolds number based on inlet diameter and Pr is the Prandtl number for room temperature air.

Uncertainties in heat transfer coefficients, calculated according to the method outlined by Kline and McClintock (ref. 8), were nominally 5 percent. Details of the inlet profiles, turbulence measurements, and uncertainty analysis can be found in reference 4. Note all heat transfer data are available online or on CD. The Uniform Resource Locators (URLs) for these files are found at the end of this report on the Report Documentation Page under "Supplementary Notes."

Duct 1

Figure 7 shows the calculated Nusselt number for an open-tunnel, low (1 percent) free-stream turbulence case for Reynolds numbers 2.26×10^6, 1.56×10^6, and 0.48×10^6. Contour patterns are similar for all Reynolds numbers, and generally the maximum heat transfer is about twice as high as the minimum values. The Nusselt number ranged from 1450 to 2750 for the 2.26×10^6 Reynolds number case, 1000 to 2100 for the 1.56×10^6 Reynolds number case, and 400 to 800 for the 0.48×10^6 Reynolds number case. Figure 8 shows the Nusselt number normalized by the correlated pipe flow Nusselt value baseline Nu_0 for the same data. For all Reynolds numbers, the heat transfer roughly matches the calculated baseline values in the round inlet section of the duct. As the top of the duct converges, the heat transfer rises above the baseline value; the heat transfer is highest, as expected, in the center of the duct where the flow impinges on the top of the duct and is diverted downward and outward. On the sides of the duct where the cross section diverges, the heat transfer level is below the straight duct baseline value. The minimum heat transfer is on the sides of the duct near the corners.

Figures 9 and 10 show Nu and Nu/Nu_0 contours, respectively, for the high (16 percent) grid-generated turbulence case at Reynolds numbers 1.42×10^6 and 0.45×10^6. Heat transfer contours are similar to the low turbulence cases except near the duct inlet where the high turbulence has increased the heat transfer. The higher turbulence also seems to have shrunk the range of maximum to minimum heat transfer. At the high Reynolds number the Nusselt number ranged from 1450 to 2050, while at the low Reynolds number the Nusselt ranged from 600 to 900. For the high turbulence cases the maximum is only about 1.5 times the minimum value compared with 2 times for the low turbulence cases. Generally, the higher turbulence did not have a large effect on the maximum heat transfer areas but did significantly raise the minimum heat transfer values.
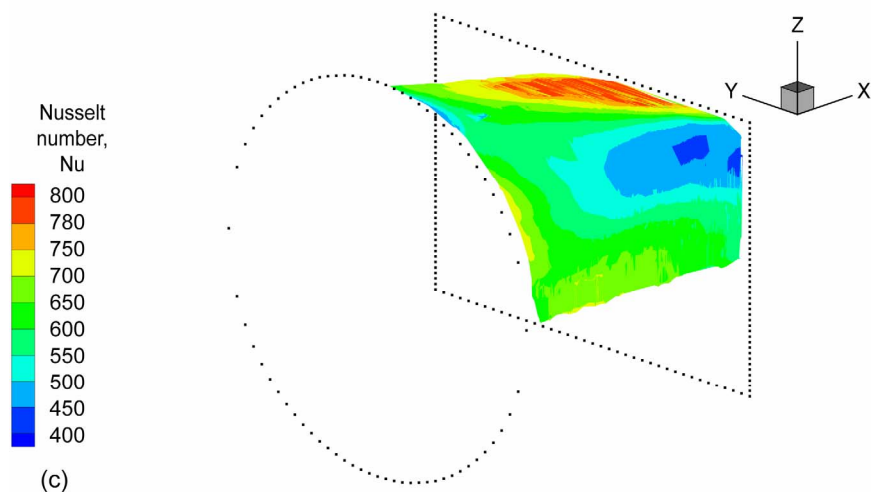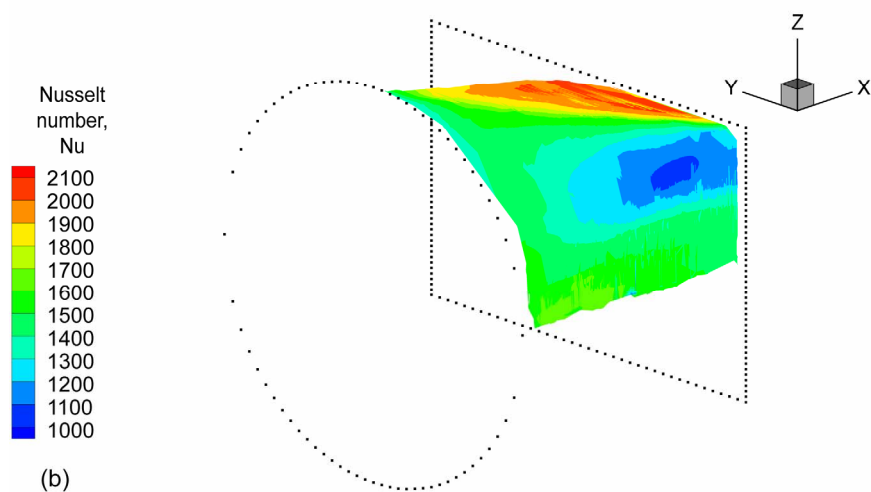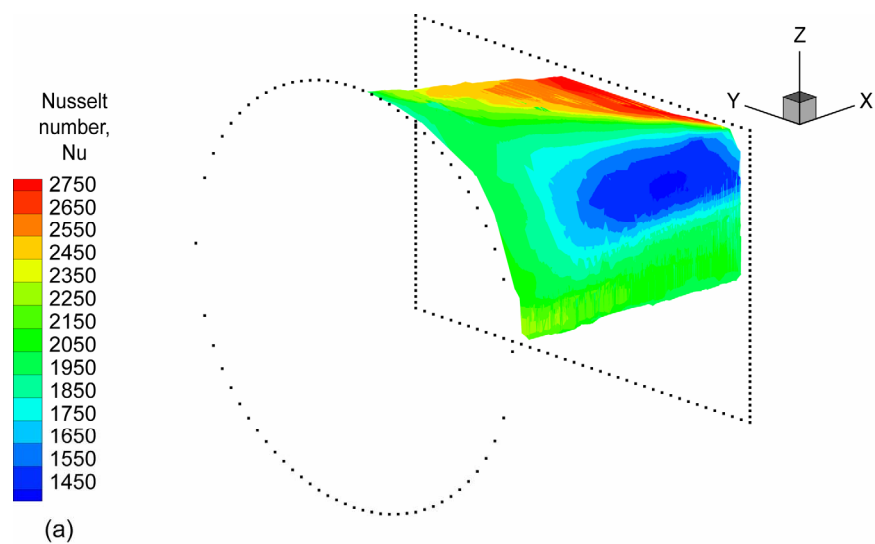
Figure 7.—Duct 1 heat transfer contours at nominal 1 percent turbulence intensity (*Tu*) for three Reynolds numbers (Re). (a) Re = 2.26×10^6. (b) Re = 1.56×10^6. (c) Re = 0.48×10^6.
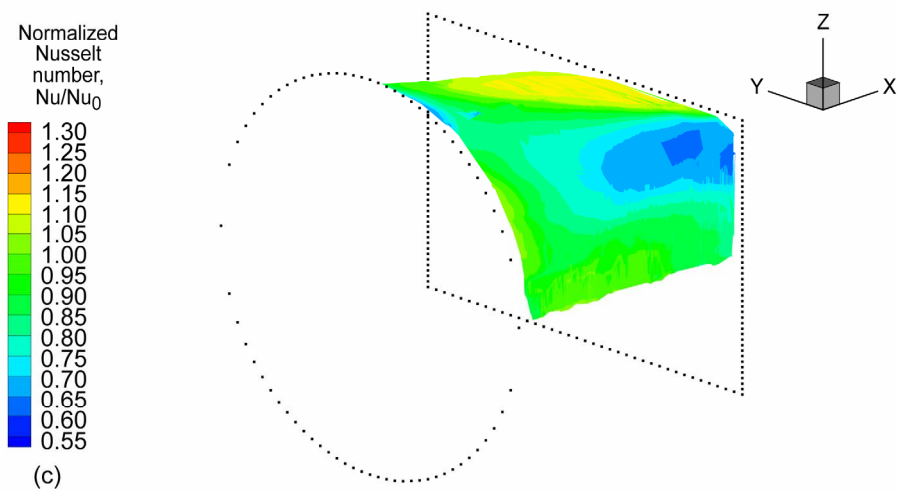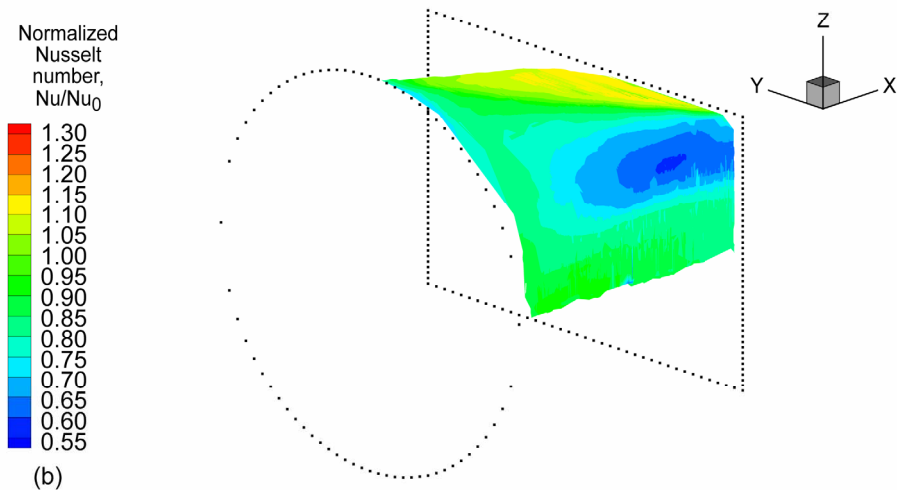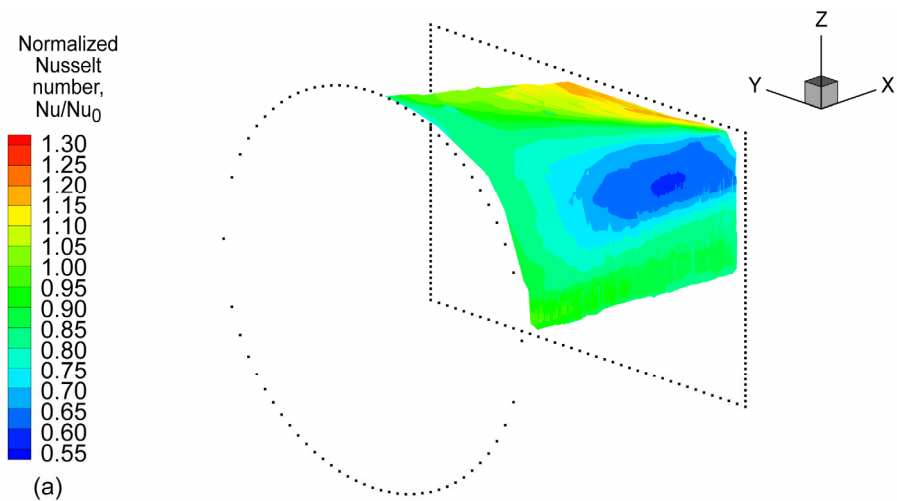
Figure 8.—Duct 1 normalized heat transfer contours at nominal 1 percent turbulence intensity (Tu) for three Reynolds numbers (Re) where Nu_0 values are Nusselt numbers for turbulent flow in a circular pipe. (a) Re = 2.26×10^6. (b) Re = 1.56×10^6. (c) Re = 0.48×10^6.
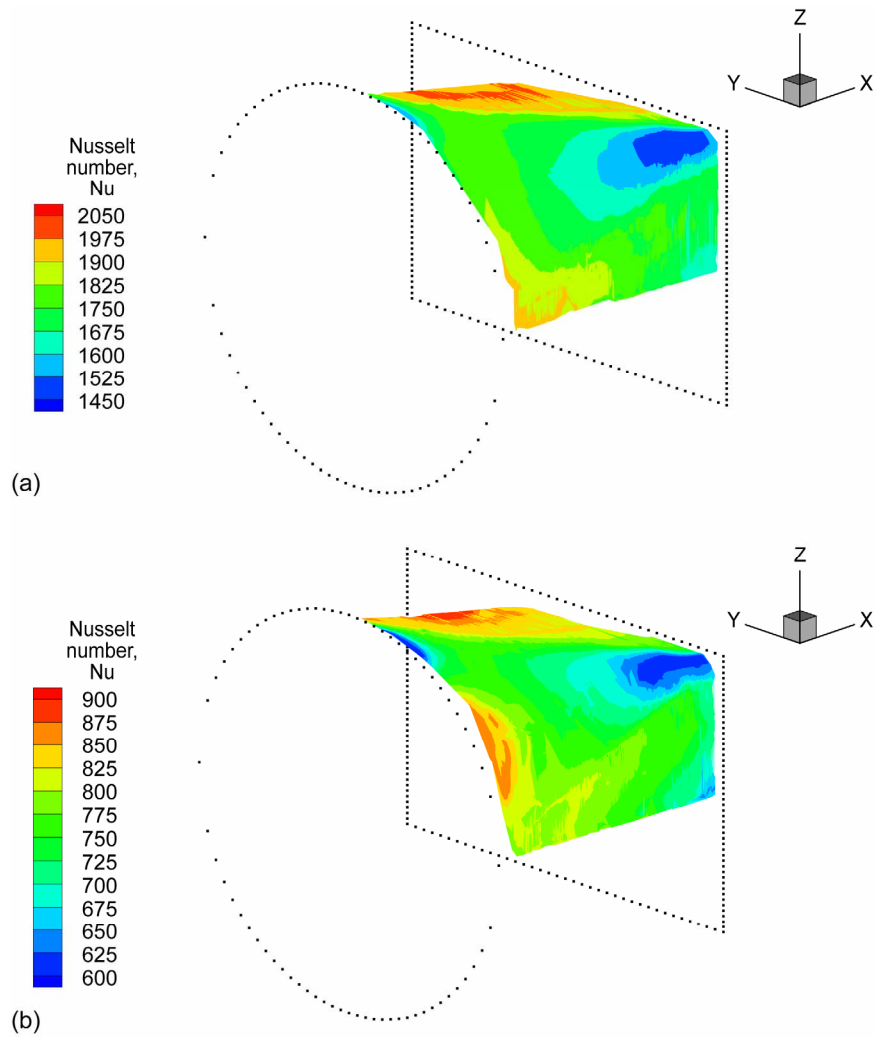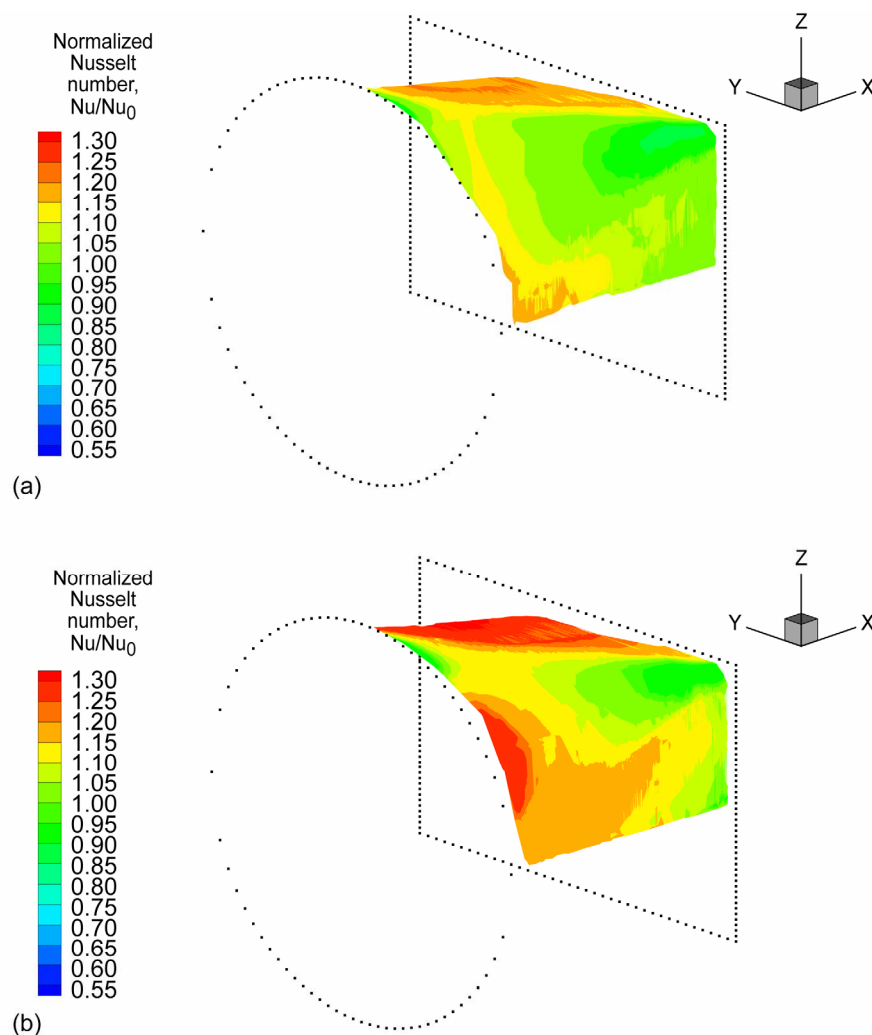
Figure 9.—Duct 1 heat transfer contours at nominal 16 percent turbulence intensity (Tu) for two Reynolds numbers (Re). (a) Re = 1.42×10^6. (b) Re = 0.45×10^6.

Figure 10.—Duct 1 normalized heat transfer contours at nominal 16 percent turbulence intensity (Tu) for two Reynolds numbers (Re) where Nu_0 values are Nusselt numbers for turbulent flow in a circular pipe. (a) Re = 1.42×10^6. (b) Re = 0.45×10^6.

Duct 2

Figure 11 shows the calculated Nusselt number for an open-tunnel low (1 percent) free-stream turbulence case for Reynolds numbers 2.39×10^6, 1.62×10^6, and 0.49×10^6. Contour patterns are similar for all Reynolds numbers. Maximum heat transfer occurs on the top where the duct surface converges, and minimum heat transfer occurs on the side where the duct diverges. A local minimum is also seen in the corners of the downstream section of the duct. For the lowest Reynolds number case, heat transfer values range from 350 to 1000, the

maximum Nusselt number being 2.9 times larger than the minimum Nusselt number. Similarly for the middle Reynolds number case, the heat transfer varies from 900 to 2700, the high Nusselt number 3.0 times larger than the low Nusselt number. Finally, the heat transfer for the high Reynolds number varies from 1100 to 3700, the high Nusselt number 3.3 times larger than the low value. Figure 12 shows Nu/Nu_0 for the same data above. Generally the heat transfer matches the baseline value on the inlet round section. The heat transfer increases to over 40 percent of the baseline at the maximum and decreases roughly 50 percent at the minimum.
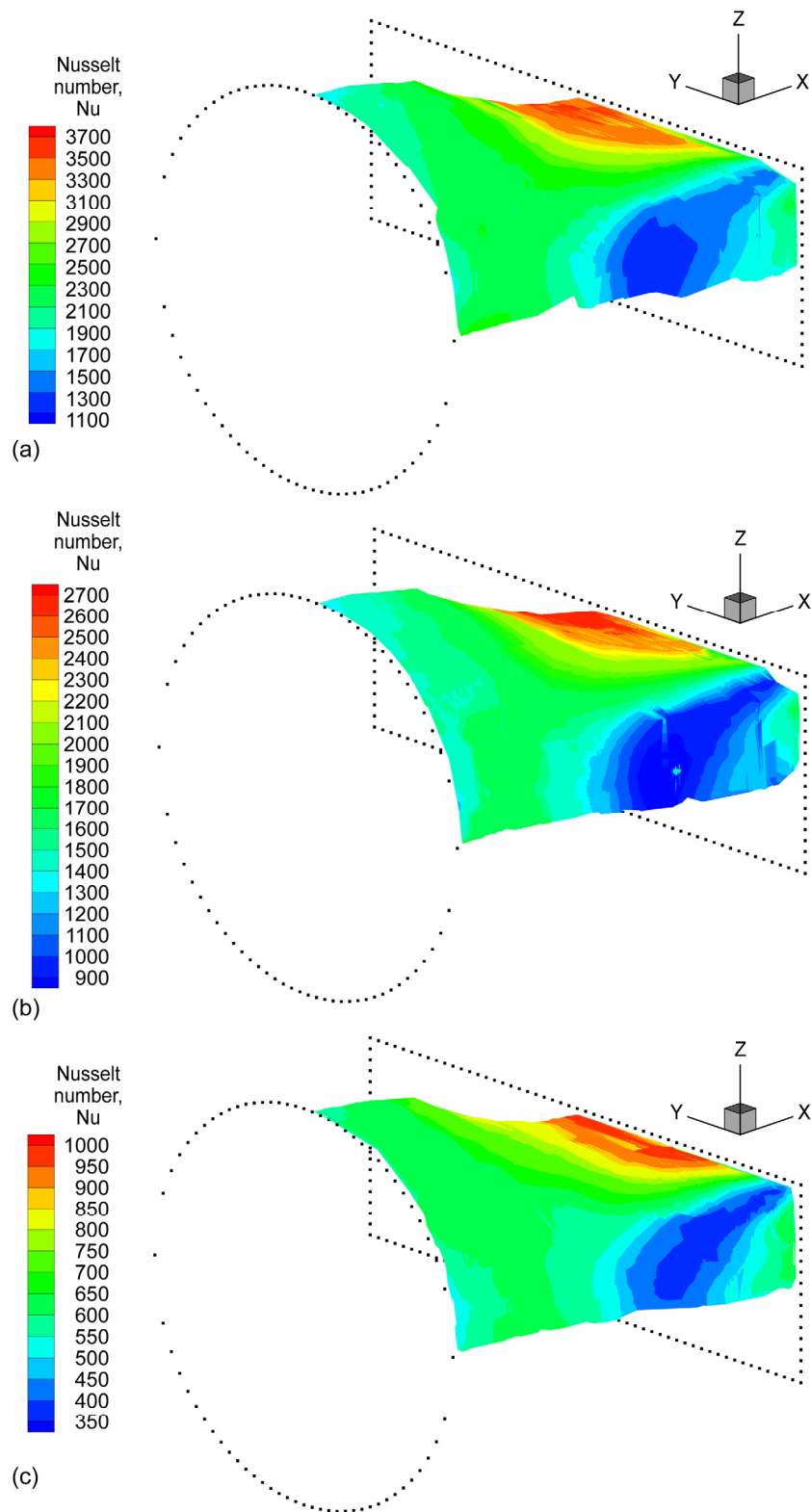
Figure 11.—Duct 2 heat transfer contours at nominal 1 percent turbulence intensity (Tu) for three Reynolds numbers (Re). (a) Re = 2.39×10^6. (b) Re = 1.62×10^6. (c) Re = 0.49×10^6.
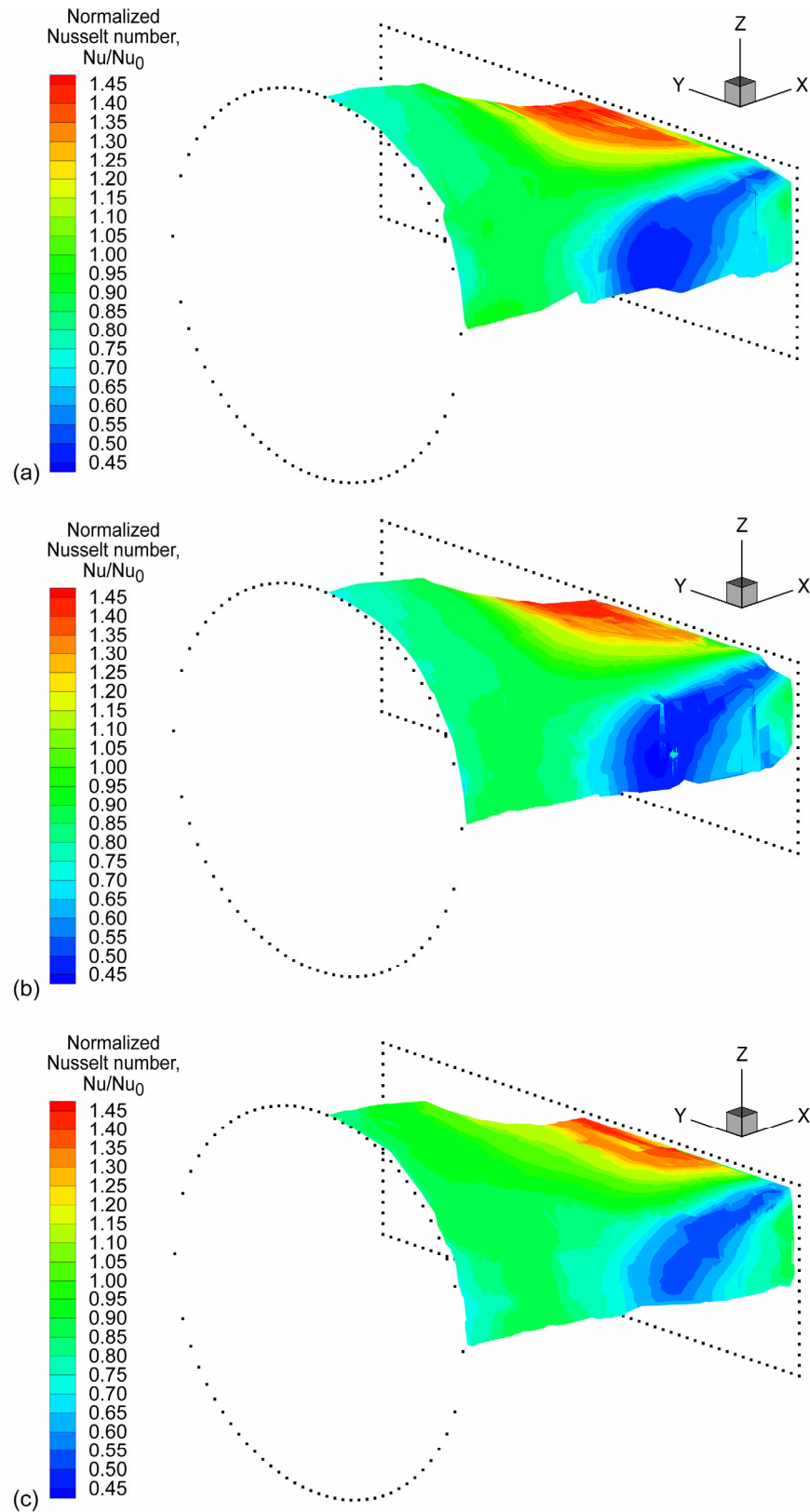
Figure 12.—Duct 2 normalized heat transfer contours at nominal 1 percent turbulence intensity (*Tu*) for three Reynolds numbers (Re) where Nu_0 values are Nusselt numbers for turbulent flow in a circular pipe. (a) Re = 2.39×10^6. (b) Re = 1.62×10^6. (c) Re = 0.49×10^6.
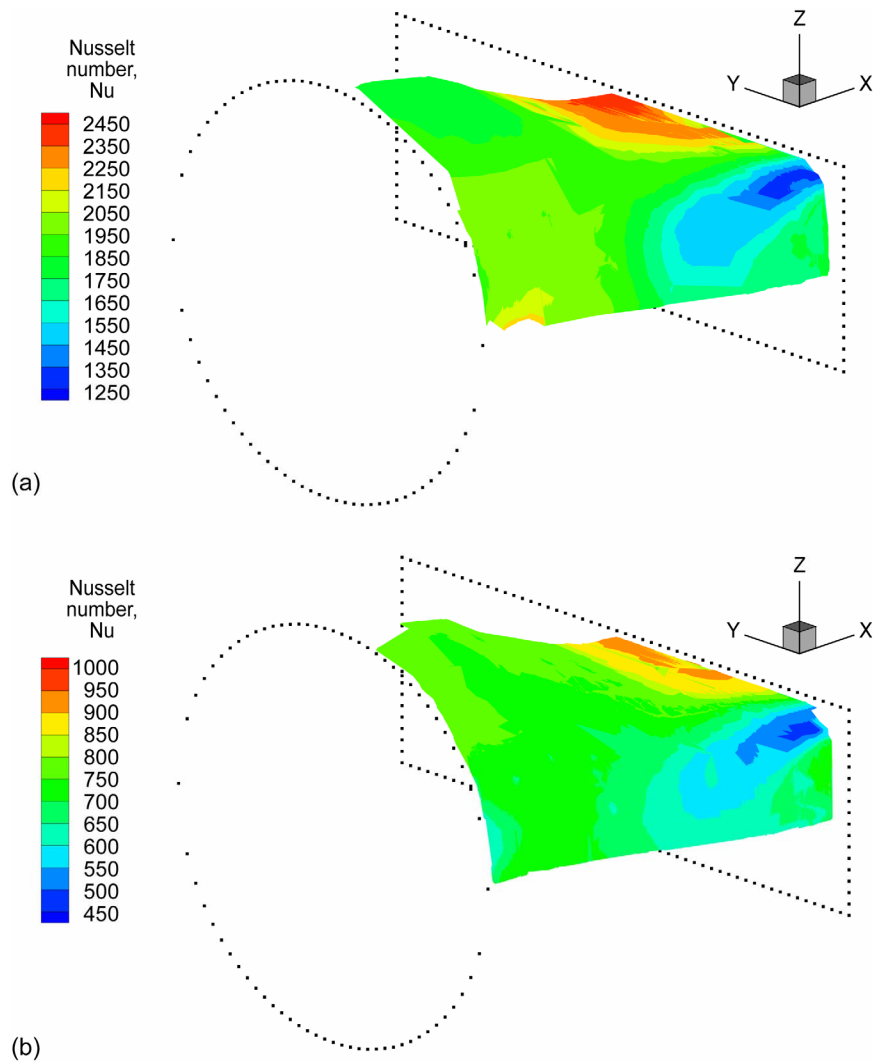
Figure 13.—Duct 2 heat transfer contours at nominal 16 percent turbulence intensity (Tu) for two Reynolds numbers (Re). (a) Re = 1.45×10^6. (b) Re = 0.45×10^6.

Figure 13 shows the calculated Nusselt number for the high (16 percent) free-stream turbulence case for Reynolds numbers 1.45×10^6 and 0.45×10^6. Compared with the low turbulence cases, the higher turbulence reduces the range of low to high heat transfer. For the 16 percent turbulence cases, the heat transfer ranges from 1250 to 2450 for the highest Reynolds number, the maximum roughly 2 times the minimum value. For the low Reynolds number, the heat transfer ranges from 450 to 1000, a ratio of slightly over 2. Additionally, the high turbulence enhances the inlet area heat transfer over the low turbulence case and pushes the minimum heat transfer further into the downstream corners. Figure 14 illustrates the Nusselt number relative to the constant cross section pipe flow heat transfer baseline. Generally the heat transfer is greater than the baseline value at the duct inlet. Downstream the Nu/Nu$_0$ ratio ranges from 0.65 at the minimum to 1.4 at the maximum.

Concluding Remarks

Surface heat transfer maps of two short circle-to-rectangle transition ducts were obtained using a transient liquid crystal technique in the Transition Duct Heat Transfer Tunnel in the Engine Research Building (ERB), SW–2, at the NASA Glenn Research Center. The heat transfer patterns on both ducts were fairly smooth. The heat transfer was generally highest at the impingement area where top and bottom walls of the duct converge. Nusselt number values at this local maximum increased to values above the straight pipe correlation. Minimum values of heat transfer were observed on the sidewalls where the flow diverges. The Nusselt number decreased to values less than the straight pipe correlation.

For both ducts, the Nu/Nu$_0$ seems roughly independent of Re, as expected. Slightly higher heat transfer values were
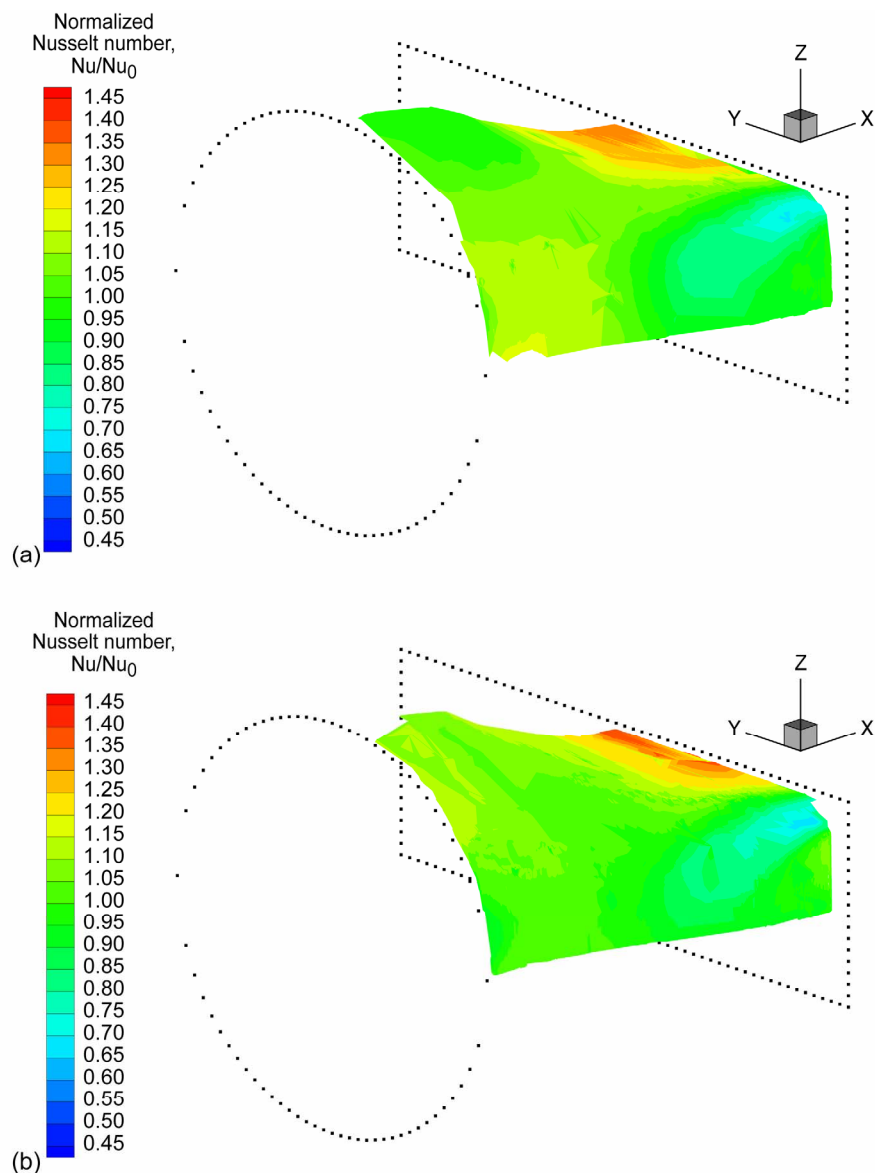
Figure 14.—Duct 2 normalized heat transfer contours at nominal 16 percent turbulence intensity (Tu) for two Reynolds numbers (Re) where Nu_0 values are Nusselt numbers for turbulent flow in a circular pipe. (a) Re = 1.45×10^6. (b) Re = 0.45×10^6.

observed on Duct 2 and a larger range of heat transfer values were seen. For Duct 1, the maximum to minimum heat transfer ratio was around 2 for low turbulence cases and around 1.5 for high turbulence cases. For Duct 2, the maximum to minimum heat transfer ratio was around 3 for low turbulence cases and around 2 for high turbulence cases.

Higher turbulence intensity generally increased the minimum heat transfer but had a lesser effect on the maximum heat transfer areas, thus the range of heat transfer values was lessened moving to higher turbulence levels.

Glenn Research Center
National Aeronautics and Space Administration
Cleveland, Ohio, June 30, 2008

References

1. Spuckler, C.: Personal communication, NASA Glenn Research Center, Cleveland, OH, 2003.
2. Buck, F.A.: Heat Transfer Tests on Circular-To-Rectangular Transition Exhaust Duct. GE R89AEB–137, 1989. Available from the Defense Technical Security Administration.

3. Patrick, William P.; and McCormick, Duane C.: Laser Velocimeter and Total Pressure Measurements in Circular-to-Rectangular Transition Ducts. United Technologies Research Center Report No. 87–41 (NASA CR–182286), 1988.

4. Poinsatte, P.E.; Thurman, D.R.; and Hippensteele, S.A.: Heat Transfer in a Superelliptic Transition Duct. NASA TM–214943, 2008.

5. Jones, T.V.; and Hippensteele, S.A.: High-Resolution Heat-Transfer-Coefficient Maps Applicable to Compound-Curve Surfaces Using Liquid Crystals in a Transient Wind Tunnel. Am. Soc. Mech. Eng. Heat Transfer Div. Publ. HTD (NASA TM–89855), vol. 71, 1987, pp. 1–9.

6. Carslaw, H.S.; and Jaeger, J.C.: Conduction of Heat in Solids. Second ed., Oxford University Press, Oxford, England, 1959.

7. Baines, W.D.; and Peterson, E.G.: An Investigation of Flow Through Screens. Trans. ASME, 1951, pp. 467–480.

8. Kline, S.J.; and McClintock, F.A.: Describing Uncertainties in Single-Sample Experiments. Mech. Eng., vol. 75, 1953, pp. 3–7.

1. REPORT DATE *(DD-MM-YYYY)* 01-06-2008	2. REPORT TYPE Technical Paper	3. DATES COVERED *(From - To)*
4. TITLE AND SUBTITLE Heat Transfer in Conical Corner and Short Superelliptical Transition Ducts		5a. CONTRACT NUMBER
		5b. GRANT NUMBER
		5c. PROGRAM ELEMENT NUMBER
6. AUTHOR(S) Poinsatte, Philip; Thurman, Douglas; Hippensteele, Steven		5d. PROJECT NUMBER
		5e. TASK NUMBER
		5f. WORK UNIT NUMBER WBS 561581.02.08.03.02.02
7. PERFORMING ORGANIZATION NAME(S) AND ADDRESS(ES) National Aeronautics and Space Administration John H. Glenn Research Center at Lewis Field Cleveland, Ohio 44135-3191		8. PERFORMING ORGANIZATION REPORT NUMBER E-16176
9. SPONSORING/MONITORING AGENCY NAME(S) AND ADDRESS(ES) National Aeronautics and Space Administration Washington, DC 20546-0001 and U.S. Army Research Laboratory Adelphi, Maryland 20783-1145		10. SPONSORING/MONITORS ACRONYM(S) NASA; ARL
		11. SPONSORING/MONITORING REPORT NUMBER NASA/TP-2008-214944; ARL-TR-4199

12. DISTRIBUTION/AVAILABILITY STATEMENT
Unclassified-Unlimited Subject Category: 34 Available electronically at http://gltrs.grc.nasa.gov This publication is available from the NASA Center for AeroSpace Information, 301-621-0390

13. SUPPLEMENTARY NOTES
Heat transfer data for Duct 1: Conical Corner are found at http://gltrs.grc.nasa.gov/reports/2008/TP-2008-214944/Duct1heattransferdata.xls and heat transfer data for Duct 2: Short Superellipse are found at http://gltrs.grc.nasa.gov/reports/2008/TP-2008-214944/Duct2heattransferdata.xls .

14. ABSTRACT
Local surface heat transfer measurements were experimentally mapped using a transient liquid-crystal heat-transfer technique on the surface of two circular-to-rectangular transition ducts. One has a transition cross section defined by conical corners (Duct 1) and the other by an elliptical equation with changing coefficients (Duct 2). Duct 1 has a length-to-diameter ratio of 0.75 and an exit plane aspect ratio of 1.5. Duct 2 has a length-to-diameter ratio of 1.0 and an exit plane aspect ratio of 2.9. Test results are reported for various inlet-diameter-based Reynolds numbers ranging from 0.45×10^6 to 2.39×10^6 and two freestream turbulence intensities of about 1 percent, which is typical of wind tunnels, and up to 16 percent, which may be more typical of real engine conditions.

15. SUBJECT TERMS
Heat transfer; Transition duct; Liquid crystal; Heat transfer coefficient

16. SECURITY CLASSIFICATION OF:			17. LIMITATION OF ABSTRACT	18. NUMBER OF PAGES	19a. NAME OF RESPONSIBLE PERSON STI Help Desk (email:help@sti.nasa.gov)
a. REPORT U	b. ABSTRACT U	c. THIS PAGE U	UU	20	19b. TELEPHONE NUMBER *(include area code)* 301-621-0390

Standard Form 298 (Rev. 8-98)
Prescribed by ANSI Std. Z39-18